THE JOURNAL OF BIOLOGICAL CHEMISTRY VOL. 286, NO. 39, pp. 34468–34478, September 30, 2011

Coupling dTTP Hydrolysis with DNA Unwinding by the DNA Helicase of Bacteriophage T7*[S]

Received for publication, July 18, 2011, and in revised form, August 11, 2011 Published, JBC Papers in Press, August 12, 2011, DOI 10.1074/jbc.M111.283796

Ajit K. Satapathy, Arkadiusz W. Kulczyk, Sharmistha Ghosh, Antoine M. van Oijen[1], and Charles C. Richardson[2]

From the Department of Biological Chemistry and Molecular Pharmacology, Harvard Medical School, Boston, Massachusetts 02115

Background: The T7 DNA helicase couples the hydrolysis of dTTP to translocation on ssDNA and the unwinding of dsDNA.
Results: Phe^{523}, positioned in a β-hairpin loop at the subunit interface, plays a role in coupling the hydrolysis of dTTP to DNA unwinding.
Conclusion: Phe^{523} contacts the displaced complementary strand and facilitates unwinding.
Significance: The mechanism of DNA unwinding by T7 DNA helicase.

The DNA helicase encoded by gene 4 of bacteriophage T7 assembles on single-stranded DNA as a hexamer of six identical subunits with the DNA passing through the center of the toroid. The helicase couples the hydrolysis of dTTP to unidirectional translocation on single-stranded DNA and the unwinding of duplex DNA. Phe^{523}, positioned in a β-hairpin loop at the subunit interface, plays a key role in coupling the hydrolysis of dTTP to DNA unwinding. Replacement of Phe^{523} with alanine or valine abolishes the ability of the helicase to unwind DNA or allow T7 polymerase to mediate strand-displacement synthesis on duplex DNA. *In vivo* complementation studies reveal a requirement for a hydrophobic residue with long side chains at this position. In a crystal structure of T7 helicase, when a nucleotide is bound at a subunit interface, Phe^{523} is buried within the interface. However, in the unbound state, it is more exposed on the outer surface of the helicase. This structural difference suggests that the β-hairpin bearing the Phe^{523} may undergo a conformational change during nucleotide hydrolysis. We postulate that upon hydrolysis of dTTP, Phe^{523} moves from within the subunit interface to a more exposed position where it contacts the displaced complementary strand and facilitates unwinding.

DNA replication requires the transient unwinding of duplex DNA to enable the DNA polymerase to have access to a single-stranded DNA (ssDNA)[3] template for base pairing during DNA synthesis. A class of enzymes termed DNA helicases mediate this unwinding of DNA by coupling the energy of hydrolysis of a nucleoside triphosphate to conformational changes in the protein for unidirectional movement along DNA. The replisome of bacteriophage T7 can be reconstituted *in vitro* by gene 5 protein (DNA polymerase), *Escherichia coli* thioredoxin (processivity factor), gene 2.5 protein (ssDNA-binding protein), and gene 4 protein (DNA helicase and DNA primase) (1, 2). The primase and helicase activities of gene 4 protein (gp4) reside in the N-terminal and C-terminal parts of the polypeptide, respectively (3). T7 DNA primase derives several benefits from its physical association with the helicase, an association that, in other replication systems, requires an association of the separately encoded proteins (2–4). The helicase domain of gp4 places it within the SF4 family of helicases (5). Like other members of this family, gp4 assembles onto ssDNA as a hexamer, an oligomerization that is facilitated by the binding of dTTP (6, 7). On ssDNA, the protein then translocates unidirectionally 5′ to 3′ by using the energy of hydrolysis of dTTP (8). Upon encountering duplex DNA, gp4 will unwind the DNA.

The crystal structure of the hexameric gp4 reveals a 6-fold symmetric ring with a central core of 25–30 Å (Fig. 1*A*) (9). Electron microscopy and biochemical studies provide strong evidence that ssDNA threads through the central core of the helicase, and it has been proposed that ssDNA transfers from one subunit to the adjacent subunit sequentially as dTTP is hydrolyzed in the intersubunit interfaces (6, 9, 10). Recent studies have also provided information on the mechanism by which the energy of hydrolysis of a nucleoside triphosphate is coupled to the unidirectional translocation of the gene 4 helicase and unwinding of duplex DNA (10–14). Unlike other DNA helicases of this family, T7 DNA helicase preferentially uses dTTP for translocation and DNA unwinding (15, 16).

For T7 DNA helicase to initiate unwinding of a duplex DNA molecule it requires a preformed fork bearing a 5′-single-stranded tail of greater than 17 nucleotides and a 3′-tail of at least 7 nucleotides (16, 17). gp4 assembles on the 5′-ssDNA tail and the 3′-tail prevents duplex DNA from entering the central core (18). A report on *E. coli* DnaB helicase provides evidence that the 3′ arm plays a role analogous to a mechanical fulcrum for the hexameric helicase bound to the 5′ arm, necessary to

* This work was supported, in whole or in part, by National Institutes of Health Grant GM54397 (to C. C. R.).
[S] The on-line version of this article (available at http://www.jbc.org) contains supplemental Figs. S1–S6.
[1] Present address: Zernike Institute for Advanced Materials Centre for Synthetic Biology, Nijenborgh 4, 9747 AG Groningen, The Netherlands.
[2] To whom correspondence should be addressed: 240 Longwood Ave., Boston, MA 02115. Tel.: 617-432-1864; Fax: 617-432-3362; E-mail: ccr@hms.harvard.edu.
[3] The abbreviations used are: ssDNA, single-stranded DNA; dsDNA, double-stranded DNA; gp5/trx, gene 5 polymerase/thioredoxin; AMPPNP, 5′-adenylyl-β,γ-imidodiphosphate.

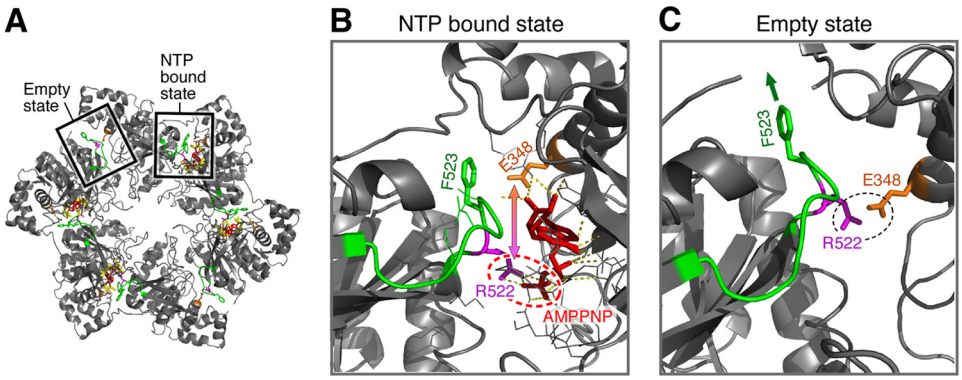

FIGURE 1. **Crystal structures of the helicase domain of T7 gp4.** *A*, crystal structure of the helicase domain of T7 gp4 (PDB code 1E0J) drawn in PyMOL. The hexameric structure provides a DNA-binding site in the central core of the ring and creates the NTP-binding site at interfaces of the subunits. One nucleotide-binding site is shown with a NTP (*sticks in red*) and another in the empty state. The subunit interface β-hairpin, the subject of this article, is colored in *green*. *B* and *C*, a magnified view of the β-hairpin from the nucleotide bound state compared with the empty state of the nucleotide binding pocket. In the nucleotide bound state, Arg^{522} interacts with the γ-phosphate of the nucleotide (AMPPNP) and Phe^{523} is partially buried at the interface. In the empty state, Arg^{522} is juxtaposed to Glu^{348} from the adjacent subunit and facilitates positioning of the Phe^{523} toward the outer surface.

provide mechanical support for the advancing helicase on the opposite strand of the DNA (19). However, the interaction site of the helicase, if any, during unwinding of DNA with the excluded strand is not known. The crystal structures of T7 DNA helicase are in the absence of DNA so it is not known if the assembly of gp4 on duplex DNA differs from that on ssDNA. Mechanistically, the interaction of the helicase with the two strands of duplex DNA during unwinding is important for differentiating whether the helicase destabilizes duplex DNA (active helicase) or opportunistically translocates onto thermally open DNA (passive helicase). In earlier studies, a random mutagenesis of gene 4 revealed residues (Ser^{345} and Gly^{451} in the helicase domain) to be important for DNA unwinding (20). Arg^{522} (the arginine finger) and Lys^{467} (central β-hairpin) mutations also lead to a loss of DNA unwinding (21, 22). It is interesting to note that each of these amino acid residues resides at the subunit interface of the hexameric gp4 and all of the mutants retain the ability to hydrolyze dTTP (supplemental Fig. S1).

From examination of the crystal structure of gp4, we have identified a β-hairpin located at the subunit interface that includes residues 522 through 530 (Fig. 1). The β-hairpin starts with the arginine finger (Arg^{522}) followed by Phe^{523} and eight other residues (Thr^{524}-Gly-Asp-Thr-Gly-Ile-Ala^{530}). This β-hairpin adopts different orientations depending upon the availability of nucleotide in the nucleotide-binding site at the subunit interface. In the presence of a nucleotide, Phe^{523} is buried within the subunit interface, and Arg^{522} contacts the γ-phosphate of the nucleotide (Fig. 1*B*). However, in the absence of a nucleotide, the β-hairpin undergoes a conformational change such that Arg^{522} makes a hydrogen bridge with Glu^{348} from the adjacent subunit and Phe^{523} is more exposed toward the exterior surface of gp4 (Fig. 1*C*). In the present study, we substituted Phe^{523} with a variety of amino acids and examined the ability of these altered helicases to support T7 growth. We also determined the biochemical properties of these helicases in isolation or in association with T7 DNA polymerase. Our results show that Phe^{523} plays a crucial role in coupling NTP hydrolysis with DNA unwinding by stabilizing the excluded strand by hydrophobic interactions.

EXPERIMENTAL PROCEDURES

Materials

E. coli C600, *E. coli* HMS174 (DE3), and pET11b were from Novagen. Wild-type and gene 4-deficient T7 phage (T7Δ4) were from the laboratory collection. Oligonucleotides were from Integrated DNA Technologies. M13 ssDNA and T4 polynucleotide kinase were from New England Biolabs. The site-directed mutagenesis kit was from Stratagene. All chemicals and reagents were from Sigma unless otherwise specified.

Methods

Phage Complementation Assays—E. coli C600 cells transformed with a plasmid that expresses gene 4 under a T7 promoter were grown to an A_{600} of 1. Serially diluted T7 phage stocks were mixed with an aliquot of the *E. coli* culture in 0.7% soft agar and poured onto LB plates with appropriate antibiotics. After incubation for 4–6 h at 37 °C, the number of plaques that appeared was counted. The number of plaques formed by plasmids harboring wild-type gp4 was normalized to 1. The relative efficiency of plating obtained with the altered gene 4 constructs was determined by the number of plaques formed by the mutated gene 4 constructs divided by the number of plaques formed of wild-type gene 4.

Mutagenesis, Overexpression, and Purification of Gene 4 Proteins—Plasmid pET11gp4-63 was used for expression and overproduction of wild-type gp4 (23). The plasmid was also used to create point mutations by using the QuikChange II Mutagenesis kit (Stratagene) in accordance with the manufacturer's instructions. The sequences of primers used to construct various single mutations are available on request. Mutations were confirmed by DNA sequencing. Constructs harboring wild-type or mutated gene 4 were transferred to *E. coli* strain HMS174 (DE3) for overproduction of the corresponding proteins. Wild-type and altered gene 4 proteins were purified as described earlier (10). The purified proteins are >95% pure as judged by Coomassie staining of the proteins on a polyacrylamide gel (supplemental Fig. S2).

dTTP Hydrolysis Assays— dTTP hydrolysis assays were carried out at 37 °C in a reaction mixture containing 40 mM Tris-

HCl (pH 7.5), 10 mM $MgCl_2$, 10 mM DTT, 50 mM potassium glutamate, 100 nM gp4, 5 nM M13 ssDNA, and the indicated concentration of [α-^{32}P]dTTP (22). After incubation for 30 min at 37 °C, EDTA was added to a final concentration of 25 mM to stop the reaction and then the reaction sample was kept on ice. The product of hydrolysis of [α-^{32}P]dNDP was separated from [α-^{32}P]dNTP on polyethyleneimine-coated TLC plates using 0.5 M formic acid and 0.5 M lithium chloride. The TLC plates were scanned in a phosphorimager (Fuji) and the intensity of the spots was measured using ImageQuant software (Fuji). The data were further analyzed using GraphPad Prism software.

DNA Binding Assays—A nitrocellulose filter-binding assay was used for measuring the ability of gp4 to bind to ssDNA or duplex DNA. Reaction mixtures (20 μl) containing either 1 nM 5′-^{32}P-labeled 95-mer oligonucleotide (5′-T_{39} GGC ATG TCA CGA CGT TGT AAA ACG ACG GCC AGT GAA TTC GAG CTC GGT ACC CGG CG-3′) or 1 nM 5′-^{32}P-labeled 95-mer oligonucleotide partially annealed to a 75-mer oligonucleotide (5′-CGC CGG GTA CCG AGC TCG AAT TCA CTG GCC GTC GTT TTA CAA CGT CGT GAC ATG CCT_{19}-3′). These DNAs were incubated with different concentrations (25–250 nM) of gp4 in 40 mM Tris-HCl (pH 7.5), 10 mM $MgCl_2$, 10 mM DTT, 50 mM potassium glutamate, and 1 mM β,γ-methylene dTTP at 37 °C for 30 min. The reaction mixtures were filtered through two layers of membranes, a nitrocellulose membrane (0.45 μM) laid above a Zeta Probe (Bio-Rad) membrane. After washing with the buffer three times, protein-DNA complex bound to the nitrocellulose membrane and free DNA bound to the Zeta Probe membrane were measured with a Fuji/BAS 1000 Bioimaging analyzer.

DNA Unwinding Assays—The substrate for DNA unwinding assays was prepared by annealing a 5′-^{32}P-end-labeled 75-mer oligo (5′-CGC CGG GTA CCG AGC TCG AAT TCA CTG GCC GTC GTT TTA CAA CGT CGT GAC ATG CCT_{19}-3′) with an unlabeled 95-mer oligo (5′-T_{39} GGC ATG TCA CGA CGT TGT AAA ACG ACG GCC AGT GAA TTC GAG CTC GGT ACC CGG CG-3′). Reaction mixtures (20 μl) containing 100 nM labeled DNA substrate, 50 nM gp4, 40 mM Tris-HCl (pH 7.5), 10 mM $MgCl_2$, 10 mM DTT, 50 mM potassium glutamate, and 1 mM dTTP were incubated at 37 °C for up to 10 min. The reactions were stopped by the addition of 0.4% (w/v) SDS, 40 mM EDTA, 8% (v/v) glycerol, and 0.1% (w/v) bromphenol blue to the final concentrations. Single-stranded oligonucleotides were separated from the duplex substrate in a 10% nondenaturing polyacrylamide gel. Image intensities were quantified using Image Gauge and GraphPad Prism software.

Protein Oligomerization Assay—gp4s were examined for their ability to oligomerize in the presence of a nonhydrolyzable dTTP analog (β,γ-methylene dTTP). The reaction mixtures (15 μl) containing 2 μM (monomer) gp4, 40 mM Tris-HCl (pH 7.5), 10 mM $MgCl_2$, 10 mM DTT, 50 mM potassium glutamate, 0.01 to 1 mM β,γ-methylene dTTP and 1 μM 50-mer ssDNA were incubated for 20 min at 37 °C. The reactions were stopped by the addition of glutaraldehyde to 0.033% (v/v). The reaction sample was kept at 37 °C for another 5 min, and the reaction products were analyzed on a nondenaturing 10% polyacrylamide gel using a running buffer of 0.25× TBE. After staining with Coomassie Blue, the oligomerization status of gp4 was determined by gel analysis as described (24). The mobility of hexamers and heptamers were distinguished as described earlier (25). The density of protein bands corresponding to monomers and higher order oligomers in each lane were measured by Alpha-Ease FC software (AlphaImager 3400). The fraction of hexamers formed from monomers was determined by the density of hexamers and higher order oligomers divided by the total density of protein bands in the corresponding lane as described earlier (26, 27). The fraction of hexamers formed was plotted against the concentration of β,γ-methylene dTTP and obtained the apparent dissociation constant (K_D) for hexamer formation (26, 27).

Strand-displacement DNA Synthesis Assays—M13 circular dsDNA having a 5′-tail was used to monitor strand-displacement DNA synthesis. A replication fork was constructed by annealing M13 ssDNA to an oligonucleotide (5′-T_{36}AAT TCG TAA TCA TGG TCA TAG CTG TTT CCT-3′) having 30 bases complementary to the M13 ssDNA and 36 bases forming a 5′-tail. Then gp5/trx was used to convert the ssDNA circle to dsDNA circle. Phenol/chloroform was used to remove gp5/trx. Strand-displacement synthesis assay was carried out at 37 °C in a 30-μl reaction mixture containing 40 mM Tris-HCl (pH 7.5), 10 mM $MgCl_2$, 10 mM DTT, 50 mM potassium glutamate, 10 nM gp5/trx, 20 nM wild-type or altered gp4 (hexamer), 500 μM each of dATP, [α-^{32}P]dTTP (10 Ci/mmol), dCTP, and dGTP, and 10 nM M13 double-stranded DNA. After incubation of the reactions up to 30 min, the reaction was stopped with EDTA at a final concentration of 25 mM and then the mixture was spotted onto DE81 filter paper. After washing 3 times with 0.3 M ammonium formate and 100% ethanol, incorporated [^{32}P]dTMP was measured in a liquid scintillating counter (28).

Single-molecule Analysis—Phage λ DNA molecules containing a replication fork were attached with the end of one strand to the glass surface of a flow cell via the biotin-SA link and with the other end to a 2.8-μm paramagnetic bead (Dynal) via digoxigenin-antidigoxigenin as described previously (29, 30). To prevent nonspecific interactions between the beads and the surface, a 1 piconewton magnetic force was applied upward by positioning a permanent magnet above the flow cell. Beads were imaged with a CCD camera with a time resolution of 500 ms, and the centers of their positions for every acquisition time point were determined by particle-tracking software. Bead-bound and surface-tethered DNA were preincubated with 100 nM T7 gp5/trx and 50 nM T7 gp4 (wild-type gp4, gp4-F523H, or gp4-F523V) in replication buffer (40 mM Tris, pH 7.5, 50 mM potassium glutamate, 2 mM EDTA, 0.1 mg/ml of BSA) with 600 μM each dNTP and 10 mM DTT for 15 min. Next, the flow cell was washed with replication buffer with dNTPs and DTT. Finally, DNA synthesis was initiated by introducing replication buffer with dNTPs, DTT, and 10 mM $MgCl_2$. After particle tracking, traces were corrected for residual instabilities in the flow by subtracting traces corresponding to tethers that were not enzymatically altered. Bead displacements were converted into numbers of nucleotides synthesized using the known length difference between ssDNA and dsDNA at our experimental conditions (29).

Physical Interaction of Proteins—Protein interactions were measured using surface plasmon resonance. Surface plasmon

TABLE 1

Plating efficiency of T7Δ4 on *E. coli* containing plasmids expressing wild-type or altered gene 4 proteins

The ability of plasmids encoding gp4 variants to support the growth of T7Δ4 in *E. coli* was examined. The number of plaques formed by plasmids harboring wild-type gp4 is normalized to 1. The relative efficiency of plating obtained with the altered gene 4 constructs was determined by the number of plaques (PFU) formed by the mutated gene 4 constructs divided by the plaque forming units of wild-type gene 4. The efficiency of plating of $\leq 10^{-9}$ corresponds to the gene 4 construct unable to complement the T7Δ4 growths in the host bacteria.

pET11b:gp4 construct	Efficiency of plating T7Δ4
Wild-type	1
F523A	$\leq 10^{-9}$
F523V	$\leq 10^{-9}$
F523I	0.9
F523L	0.8
F523H	0.9
F523Y	0.8

resonance was performed using a Biacore 3000 instrument. Wild-type or altered gp4 were immobilized (3000 response units) on a CM-5 (carboxymethyl-5) chip using EDC/NHS chemistry. Immobilization was performed in 10 mM sodium acetate (pH 5.0) at a flow rate of 10 μl/min. Binding studies were performed in 20 mM HEPES (pH 7.5), 10 mM $MgCl_2$, 250 mM potassium glutamate, 5 mM DTT, at a flow rate of 40 μl/min (30). The chip surface was regenerated using 1 M NaCl at a flow rate of 100 μl/min. As a control, a flow cell was activated and blocked in the absence of protein to account for changes in the bulk refractive index. gp5/trx (0.1 to 3 μM) was flowed over the bound gp4 as shown in the Fig. 7*A*. Apparent binding constants were calculated under steady-state conditions and the data were fitted using BIAEVAL 3.0.2 software (Biacore).

To examine the binding of gp5/trx to gp4 in the presence of primer-template, biotinylated DNA was coupled to a streptavidin-coated chip as previously described (see Fig. 7*B*). A template strand was used with a biotin group attached to 3′-end, and an annealed primer (30). The template DNA was coupled at a concentration of 0.25 μM in HBS-EP buffer (10 mM HEPES (pH 7.4), 150 mM NaCl, and 0.005% (v/v) Tween 20) at a flow rate of 10 μl/min. Binding studies of gp5/trx were performed in 20 mM HEPES (pH 7.4), 5 mM $MgCl_2$, 2.5 mM DTT, 200 mM potassium glutamate, and 1% (w/v) glycerol at a flow rate of 10 μl/min. gp5/trx was injected at a concentration of 0.2 μM in a flow buffer containing 1 mM dGTP and 10 μM ddATP: a saturating 1:1 binding condition between gp5/trx and primer-template. gp4 was injected over the chip in the above buffer containing 0.1 mM ATP and 2 mM dGTP. A flow cell blocked with biotin was used as a control to measure nonspecific interaction and bulk refractive index of the sample buffer containing gp4. The chip surface was stripped of bound proteins by sequential injections of 150 μl of 1 M NaCl at a flow rate of 100 μl/min.

RESULTS

Phe^{523} Is Required for T7 Phage Growth—The effect of the genetically altered gene 4 proteins on the growth of T7 phage was examined (Table 1). T7Δ4 phage, lacking gene 4, are dependent on the expression of plasmid-encoded gene 4 protein for viability (31). To ascertain the role of Phe^{523}, gene 4 mutants were constructed in which Phe^{523} was replaced with alanine (gp4–523A), valine (gp4–523V), isoleucine (gp4–523I), leucine (gp4–523L), histidine (gp4–523H), or tyrosine (gp4–523Y). Plasmids encoding gp4-F523I, gp4-F523L, gp4-F523H, and gp4-F523Y complemented the growth of T7Δ4 with similar levels of efficiency of plating as wild-type gp4 (Table 1). In contrast, gp4-F523A and gp4-F523V did not support the growth of T7Δ4 phage. Wild-type T7 phage grow normally in the presence of these altered helicases.

Role of Phe^{523} in ssDNA-dependent dTTP Hydrolysis—The proteins coded by Phe^{523}-altered constructs were overproduced, purified, and characterized biochemically. To determine whether Phe^{523} plays a role in DNA-dependent hydrolysis of dTTP, we measured dTTP hydrolysis activity of the gene 4 proteins in the presence of M13 ssDNA (Fig. 2). All of the altered proteins had DNA-dependent dTTP hydrolysis activity albeit with reduced efficiency. The kinetic parameters of these assays are presented in Table 2. gp4-F523A, gp4-F523V, and gp4-F523H exhibited about 20–30% of dTTP hydrolysis activity. However, only gp4-F523H complemented the growth of T7Δ4 phage. gp4-F523I, gp4-F523L, and gp4-F523Y exhibited 60–70% of dTTP hydrolysis activity as compared with that of wild-type gp4 and all of them complemented gene 4 function *in vivo*. Despite the differences in the maximal rate of dTTP hydrolysis activity among the Phe^{523}-altered helicases, the calculated k_{cat}/K_m values for each of these proteins are comparable with the wild-type gp4 (7.6 s^{-1} mM^{-1}). In the absence of ssDNA gp4 hydrolyzes dTTP at a significantly slower rate (10) and this observation also is true for the altered proteins (Table 2). All of the proteins have significant activity in the absence of ssDNA although there is a considerable variation in the ability of the altered gp4 to hydrolyze dTTP. Altogether, results show that Phe^{523}-altered proteins retained dTTP hydrolysis activity.

Furthermore, we have measured the effect of ssDNA concentration on DNA-dependent dTTP hydrolysis (Fig. 2*B* and Table 2). All of the altered gp4 (except gp4-F523A and gp4-F523V) bind M13 ssDNA with a K_D of 0.1–0.3 nM, a value comparable with that observed with wild-type gp4 (K_D = 0.1 nM). gp4-F523A and gp4-F523V bind M13 ssDNA relatively less tightly than does wild-type gp4 with a K_D of 0.5 and 0.9 nM, respectively. This weaker binding affinity could account for the lower rate of dTTP hydrolysis activity by gp4-F523A and gp4-F523V. However, the lower rate of dTTP hydrolysis catalyzed by gp4-F523H cannot be explained in this experiment.

Role of Phe^{523} in DNA Unwinding—Upon binding of dTTP, Phe^{523} in the β-hairpin is located in the NTP-binding site. In the empty state Phe^{523} is oriented toward the outer surface of the helicase (Fig. 1). This reorientation suggests a role for Phe^{523} in helicase activity. Initially, the altered proteins were compared with wild-type gp4 for their ability to unwind dsDNA with a replication fork at one end. Wild-type gp4 will initiate unwinding on a duplex DNA molecule provided a preformed replication fork is present at one end of the DNA. The preformed fork consists of a 5′-single-stranded tail of 39 nucleotides and a 3′-single-stranded tail of 19 nucleotides (Fig. 3*A*). On this DNA gp4 can assemble on the 5′-tail and initiate unwinding, whereas it cannot on a DNA molecule having only a 3′- or 5′-tail or a blunt end (Fig. 3*A*). In this assay one strand of the duplex is labeled at its 5′ terminus with ^{32}P, which is released as ssDNA in unwinding by the helicase. Duplex and

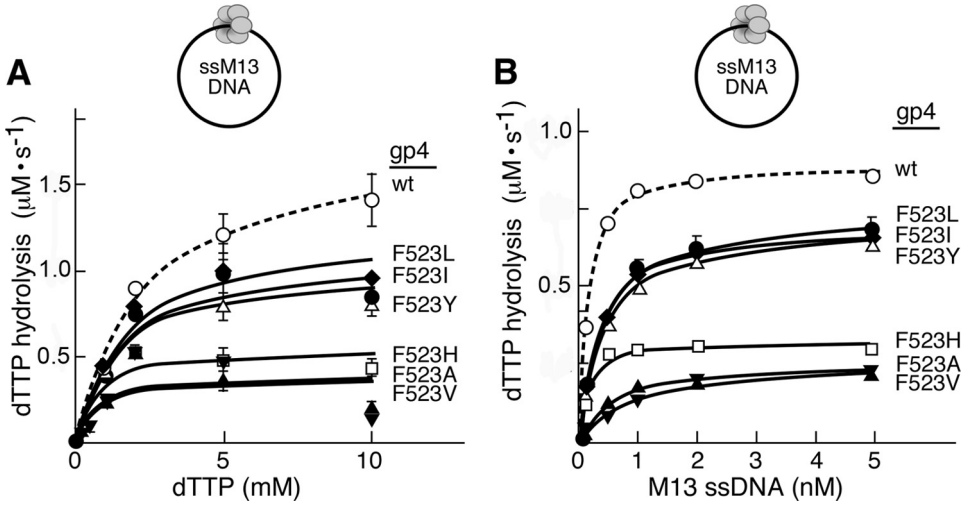

FIGURE 2. **dTTP hydrolysis activity of Phe^{523} altered gp4.** *A*, the rate of dTTP hydrolysis activity by gp4 variants was measured as a function of dTTP concentration in the presence of circular M13 ssDNA. Reactions contained 100 nM wild-type or altered gp4, 5 nM M13 ssDNA, the indicated concentrations of [α-^{32}P]dTTP, 40 mM Tris-HCl (pH 7.5), 10 mM $MgCl_2$, 10 mM DTT, and 50 mM potassium glutamate. After incubation at 37 °C for 30 min the reaction was stopped by the addition of EDTA to a final concentration of 25 mM. Separation of [α-^{32}P]dTDP from [α-^{32}P]dTTP was carried out on TLC paper coated with polyethyleneimine in a buffer containing 0.5 M lithium chloride and 0.5 M formic acid. The rate of dTTP hydrolysis activity for each of the proteins is plotted against the concentration of [α-^{32}P]dTTP used in the corresponding reactions. The maximal rate of dTTP hydrolysis (V_{max}) was calculated using the Michealis-Menten equation with the help of GraphPad Prism software. *B*, the rate of dTTP hydrolysis activity was monitored as a function of M13 ssDNA concentration. Reactions contained 100 nM wild-type or altered gp4, 5 mM [α-^{32}P]dTTP and M13 ssDNA (concentrations range from 0 to 5 nM), and were carried out as described for *A*. The K_D of gp4 variants for M13 ssDNA was determined from the graph. Please note that in all cases less than 30% of the dTTP is hydrolyzed in 30 min for each of the concentrations examined.

TABLE 2

dTTP hydrolysis activity of wild-type gp4 and the gp4 variants

The rate of dTTP hydrolysis by wild-type gp4 and gp4 variants in the presence or absence of ssDNA is compared. dTTP hydrolysis reactions were performed as described under "Experimental Procedures." Wild-type gp4 hydrolyzes dTTP approximately 75-fold faster in the presence of 5 nM M13 ssDNA as compared to the absence of DNA. The relative dTTP hydrolysis by the gp4 variants were compared with the wild-type activity. The K_{DNA} was calculated from the Fig. 2*B*.

gp4-helicase	No M13 ssDNA				5 nM M13 ssDNA				
	k_{cat}	K_m	k_{cat}/K_m	Relative k_{cat}	k_{cat}	K_m	k_{cat}/K_m	Relative k_{cat}	K_{DNA}
	s^{-1}	mM	s^{-1} mM^{-1}		s^{-1}	mM	s^{-1} mM^{-1}		nM
Wild-type	0.24 ± 0.02	0.07 ± 0.02	3.4	100	17.6 ± 1	2.3 ± 0.3	7.6	100	0.14
F523A	0.07 ± 0.01	0.2 ± 0.01	0.35	29	3.9 ± 0.7	0.5 ± 0.3	7.8	22	0.54
F523V	0.12 ± 0.01	0.2 ± 0.03	0.6	50	3.7 ± 0.8	0.5 ± 0.3	7.4	21	0.91
F523I	0.15 ± 0.02	0.3 ± 0.02	0.5	62	12.4 ± 1.2	1.6 ± 0.4	7.7	70	0.29
F523L	0.35 ± 0.03	0.2 ± 0.03	1.75	145	10.8 ± 0.9	1.3 ± 0.3	8.3	61	0.38
F523H	0.12 ± 0.01	0.1 ± 0.01	1.2	50	5.4 ± 0.4	0.5 ± 0.1	10.8	31	0.13
F523Y	0.63 ± 0.04	0.2 ± 0.04	3.15	262	9.9 ± 0.8	1.1 ± 0.3	9	56	0.37

ssDNA can be identified by electrophoresis through nondenaturing polyacrylamide gels (Fig. 3*B*). Using the DNA molecule with the preformed replication fork we find that gp4-F523A, and gp4-F523V, does not catalyze unwinding of the DNA. Interestingly, despite the reduced levels (~30%) of dTTP hydrolysis, gp4-F523H exhibited the highest level of unwinding activity (~70%) among all the Phe^{523} altered proteins. gp4-F523I, gp4-F523L, and gp4-F523Y can unwind the DNA but not as efficiently as wild-type gp4. Although gp4-F523I retains 30% of the activity of wild-type gp4, gp4-F523L and gp4-F523Y retain up to 50%, as calculated from the exponential phase of the reactions. These results demonstrate that small residues like alanine and valine cannot substitute for phenylalanine. However, hydrophobic residues with longer side chains like leucine and isoleucine can partially substitute, and amino acids with aromatic side chains such as tyrosine and histidine approach the efficiency of phenylalanine for unwinding activity. gp4-F523A and gp4-F523V did not exhibit DNA unwinding activity even at higher protein concentrations (2 μM) (supplemental Fig. S3). It is clear from these results that Phe^{523} is important in DNA unwinding by T7 DNA helicase.

Binding of Gp4 to ssDNA and at a Fork on Duplex DNA—gp4-F523A and gp4-F523V are completely defective and gp4-F523I is partially defective in unwinding duplex DNA although the later protein retains a considerable level of dTTP hydrolysis activity. One explanation for the defect in unwinding of duplex DNA is an altered interaction of the phenylalanine-substituted gp4 with the DNA at the fork to which it binds. We have measured the affinity of wild-type gp4 and the variant gp4s to both ssDNA and duplex DNA bearing a fork (Table 3). Wild-type helicase binds ssDNA and dsDNA with K_D of 16 and 9 nM, respectively. gp4-F523A binds ssDNA and dsDNA with the K_D value calculated to be ~15-fold higher than wild-type gp4. gp4-F523V and gp4-F523I bind to ssDNA ~4–6-fold weaker than wild-type gp4. In similar experiments gp4-F523V and gp4-F523I were shown to have higher K_D values for dsDNA; ~16- and 8-fold higher than wild-type protein. gp4-F523L, gp4-F523H, and gp4-F523Y did not exhibit any significant differences in binding ssDNA or dsDNA as compared with wild-

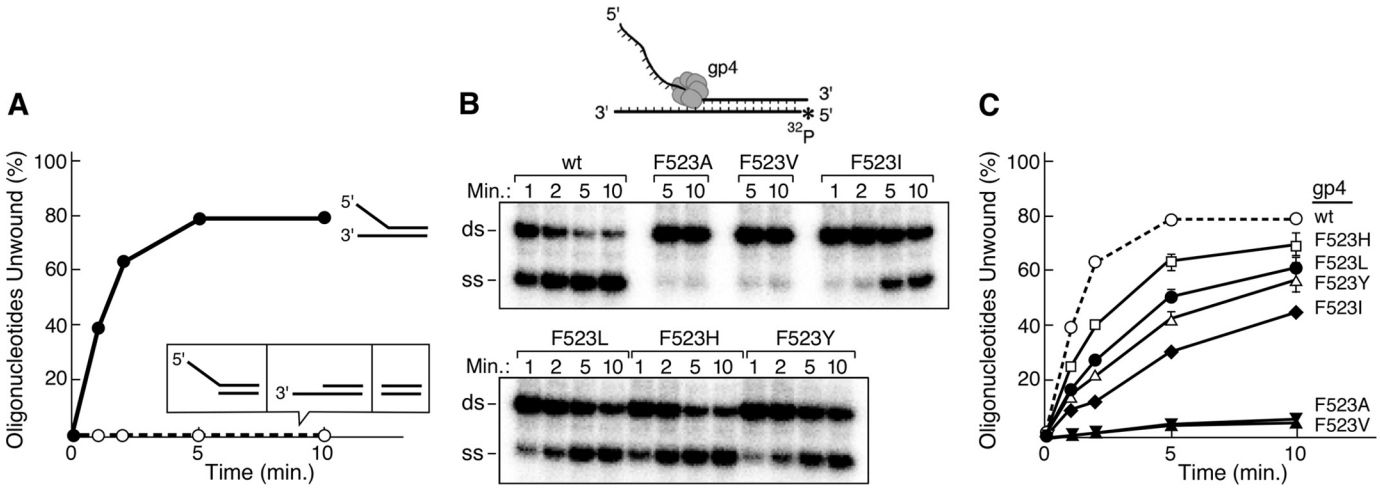

FIGURE 3. **DNA unwinding activity of gp4 with substitutions for Phe^{523}.** *A*, four different duplex DNAs, each with a different terminus, were examined for their ability to be unwound by wild-type gp4. gp4 unwinds the duplex containing both a single-stranded 3′- and 5′-tail but not those bearing a blunt end, a 5′-tail, or a 3′-tail. The reactions contained 50 nM wild-type gp4 and 100 nM DNA substrates as depicted in the figure. Incubation was at 37 °C for the indicated times and the reactions were carried out as described under "Experimental Procedures." *B*, DNA unwinding activity of gp4 variants with Phe^{523} substitutions compared with that of wild-type gp4. The DNA substrate contains a replication fork at one end allowing gp4 to assemble on the 5′-single-stranded tail (see *inset*). The reactions were carried out as described under "Experimental Procedures." The reactions contained 50 nM gp4, 100 nM DNA, and 1 mM dTTP. After incubation at 37 °C the reaction was stopped at the indicated time points. The unwound ssDNA was separated from the dsDNA substrate in a 10% nondenaturing polyacrylamide gel. The identities of each of the gp4 variants are indicated. The separation of unwound ssDNA from the dsDNA substrate can be seen from the gel picture. The band intensities in each case were measured and plotted in the graph shown in *C*. *C*, the percentage of ssDNA unwound from 100 nM substrate by wild-type or altered gp4s was plotted against the time of reaction. *Error bars* represent the standard deviation of the results from three independent experiments.

TABLE 3

Binding of gp4 helicases to ssDNA and forked-end duplex DNA

The dissociation constants for the wild-type or altered gp4s were determined in a nitrocellulose DNA-binding assay. The reactions were carried out in a 20-μl volume containing a range of concentrations of gp4, 1 nM 5′-^{32}P-labeled 95-mer ssDNA or 1 nM forked-end duplex DNA (5′-^{32}P-labeled 75-mer annealed with a cold 95-mer), 1 mM β,γ−methylene dTTP and incubated for 30 min at 37 °C as described under "Experimental Procedures." The reaction mixture was filtered through a nitrocellulose membrane laid above a Zeta Probe membrane in a dot-blot filtration apparatus. The quantity of protein bound single-stranded DNA and free single-stranded DNA was measured by scanning the nitrocellulose and Zeta Probe membrane, respectively, in a phosphorimager. The relative binding by the gp4 variants to both the substrates were compared with the wild-type activity. K_D of wild-type gp4 to bind ssDNA/dsDNA was considered as 1 and the relative binding was calculated as number of folds weaker in DNA binding by the gp4 variant.

	ssDNA (95-mer)		Forked-end dsDNA (95 + 75-mer)	
Gp4-helicase	K_D	Relative binding	K_D	Relative binding
	nM		nM	
Wild-type	16 ± 8	1	9 ± 1	1
F523A	241 ± 15	15	157 ± 86	17
F523V	101 ± 35	6	144 ± 48	16
F523I	63 ± 13	4	69 ± 7	8
F523L	17 ± 1	1	16 ± 2	2
F523H	34 ± 15	2	21 ± 5	2
F523Y	12 ± 2	1	9 ± 3	1

type gp4 (Table 3). These results show that valine can substitute for phenylalanine for binding ssDNA but not for binding at a fork on dsDNA. The increase in the size of the functional group from valine to isoleucine or leucine increases the affinity of the protein to bind the fork on dsDNA, an increase that parallels with their unwinding activity. Histidine or tyrosine can also replace Phe^{523} with no significant defect in binding to ssDNA or to the fork on dsDNA. Again these proteins show only a marginal loss in unwinding activity.

Oligomerization of gp4—The functional form of T7 DNA helicase is a hexamer. Although gp4 is found in the form of hexamers and heptamers in solution only hexamers are found to bind to DNA (25). Nucleotides play an essential role in the formation of stable hexamers. Wild-type gp4 monomers or dimers convert to the hexamer species in the presence of dTTP (26). At saturated concentrations of β,γ-methylene dTTP and ssDNA, wild-type gp4, and altered gp4s do not show any significant difference in forming hexamers even at low concentrations of protein (supplemental Fig. S5). Furthermore, the ability of the altered gp4 to oligomerize was measured on a 50-mer oligonucleotide in the presence of various concentrations of β,γ-methylene dTTP (0.01 to 1 mM) (Fig. 4*A*). The results from this ligand-dependent oligomeric assay show that gp4-F523A and gp4-F523V are relatively defective in forming hexamers at lower concentrations of β,γ-methylene dTTP (Fig. 4, *A* and *B*). The apparent K_D values in terms of concentration of β,γ-methylene dTTP for hexamer formation by gp4-F523A and gp4-F523V are 8.4 and 6.3 μM, respectively, as compared with that of the wild-type K_D value (1.2 μM) (27). gp4-F523I exhibits a K_D of 3.5 μM for hexamer formation. However, gp4-F523L, gp4-F523H, and gp4-F523Y exhibit comparable K_D values with wild-type gp4 to form hexamers and higher order oligomers (Fig. 4*C*). Despite showing defects for forming hexamers at lower nucleotide concentrations, all Phe^{523}-altered helicases including gp4-F523A and gp4-F523V form more than 90% hexamers at 1 mM β,γ-methylene dTTP. At this concentration of dTTP, gp4-F523A and gp4-F523V did not exhibit any DNA unwinding activity; however, other Phe^{523}-altered helicases exhibit unwinding activity perhaps based on the length or size of the side chain of the amino acid replaced for phenylalanine. Thus, the severe defects in DNA unwinding by gp4-F523A and gp4-F523V cannot be attributed solely to the differences in the ability of these proteins to form hexamers or higher order oligomers.

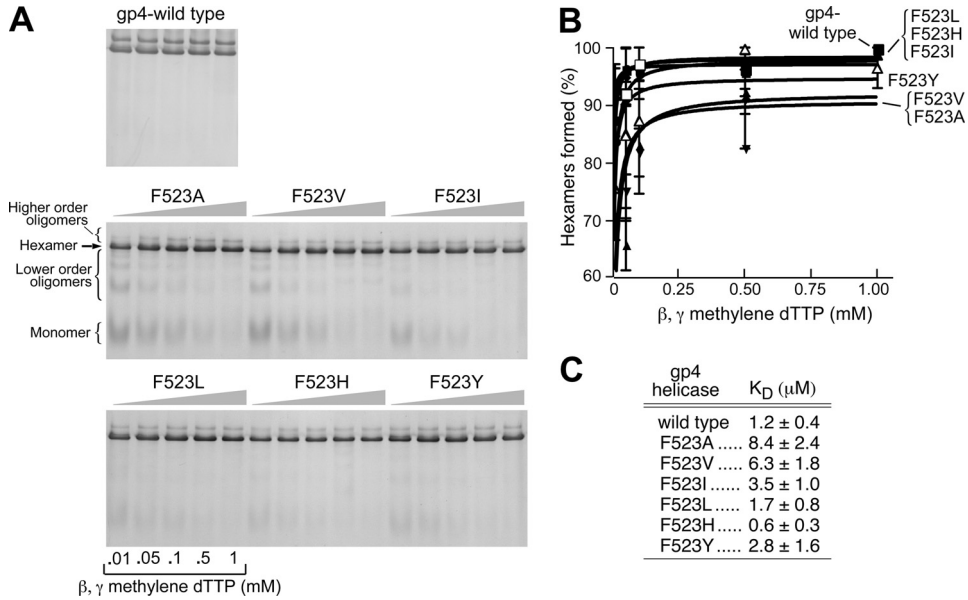

gp4 helicase	K_D (μM)
wild type	1.2 ± 0.4
F523A	8.4 ± 2.4
F523V	6.3 ± 1.8
F523I	3.5 ± 1.0
F523L	1.7 ± 0.8
F523H	0.6 ± 0.3
F523Y	2.8 ± 1.6

FIGURE 4. **Oligomerization of wild-type and Phe^{523}-altered gp4.** *A*, oligomerization reactions contained 2 μM wild-type or altered proteins, 0.01–1 mM β,γ-methylene dTTP, and 1 μM 50-mer oligonucleotide and incubated at 37 °C for 20 min as described under "Experimental Procedures." Glutaraldehyde was added to 0.033% to stabilize the oligomeric forms. The proteins were analyzed by electrophoresis on a 10% nondenaturing polyacrylamide gel. The state of the oligomerization of the proteins was determined after staining the gel with Coomassie Blue. The formation of hexamers, higher order oligomers, and lower order oligomers are shown in the gel picture. The identity of the protein is also indicated in the gel picture. *B*, fraction of hexamers and higher order oligomers formed by each of the proteins in the presence of different concentrations of β,γ-methylene dTTP are quantitated by the software AlphaEase FC (AlphaImager 3400) and plotted the graph. The *error bars* represent the standard deviation of the result from three independent experiments. *C*, calculated apparent K_D from *B* for the wild-type or Phe^{523}-altered proteins to form hexamers and higher order oligomers in the presence of β,γ-methylene dTTP and 50-mer oligonucleotide.

Strand-displacement DNA Synthesis Mediated by gp4 and T7 DNA Polymerase (gp5/trx)—T7 gene 5 protein functions *in vivo* in a 1 to 1 complex with its processivity factor, *E. coli* thioredoxin. This gene 5 polymerase/thioredoxin (gp5/trx) complex catalyzes processive DNA synthesis on ssDNA templates but is unable to catalyze strand-displacement DNA synthesis on duplex DNA (32, 33). However, in the presence of T7 DNA helicase, T7 gp5/trx mediates extensive strand-displacement DNA synthesis, a process that mimics leading strand DNA synthesis at a replication fork (34, 35). The ability of the altered helicases to support strand-displacement synthesis with gp5/trx was measured using circular M13 dsDNA bearing a 5′-ssDNA tail onto which gp4 can assemble. As anticipated, wild-type gp4 enables gp5/trx to mediate strand-displacement synthesis (Fig. 5*A*). gp4-F523I, gp4-F523L, and gp4-F523Y support strand-displacement DNA synthesis, albeit at a reduced rate (~45–55% as compared with wild-type gp4) (Fig. 5*A*). gp4-F523H retains ~75% of the wild-type activity. gp4-F523A and gp4-F523V, devoid of unwinding activity, do not support strand-displacement synthesis.

The dTTP hydrolysis activity that accompanies DNA unwinding and strand-displacement synthesis in these reactions was also measured (Fig. 5*B*). As a control dTTP hydrolysis was also measured during translocation of gp4 on M13 ssDNA in the presence of gp5/trx (Fig. 5*C*). Not surprising in view of their inability to mediate strand-displacement synthesis with gp5/trx, neither gp4-F523A nor gp4-F523V hydrolyzes dTTP on M13 dsDNA (Fig. 5*B*). However, as shown in Fig. 2 they do hydrolyze dTTP on ssDNA at ~25% that observed with wild-type gp4; the presence of gp5/trx does not have any effect in these reactions (Fig. 5*C*). gp4-F523Y hydrolyzes dTTP at a faster rate than wild-type gp4 on M13 ssDNA, but retains only 50% of the rate of wild-type activity on M13 dsDNA. The results suggest that the dTTP hydrolysis activity on M13 ssDNA depends only on the translocation activity of the protein. However, dTTP hydrolysis in the presence of M13 dsDNA accompanies unwinding in conjunction with T7 gp5/trx. Therefore gp4-F523A and gp4-F523V retaining the ability to translocate on ssDNA, however, are defective in unwind dsDNA. The experiments also show that gp4-F523H exhibit dTTPase activity parallel to its unwinding rate in conjunction with gp5/trx at the replication fork progression (Fig. 5*B*).

Single-molecule Analysis of Strand-displacement Synthesis Mediated by gp4 and T7 gp5/trx—gp4-F523H complements for T7Δ4 phage growth and the purified protein mediates leading strand synthesis in association with T7 gp5/trx. However, gp4-F523H has only 30% of the DNA-dependent dTTP hydrolysis activity but exhibit 75% of the strand-displacement activity as compared with that of wild-type helicase. On the other hand gp4-F523A and gp4-F523V also retains a considerable level of dTTP hydrolysis activity (20%), but are significantly defective in DNA unwinding and strand-displacement synthesis activity. Earlier we found that gp4-K467A, an altered gp4 with an alanine substituted a lysine in the central β-hairpin, has 15% of the wild-type rates of dTTP hydrolysis activity but no significant unwinding activity (22). However, gp4-K467A complements for gp4 function *in vivo*. By using single-molecule techniques we showed that gp4-K467A can support T7 DNA polymerase for leading strand synthesis at a rate comparable with that observed with wild-type gp4. In the present study, we have examined the wild-type gp4 and the altered proteins: gp4-F523H and gp4-F523V for T7 gp5/trx-mediated leading strand synthesis.

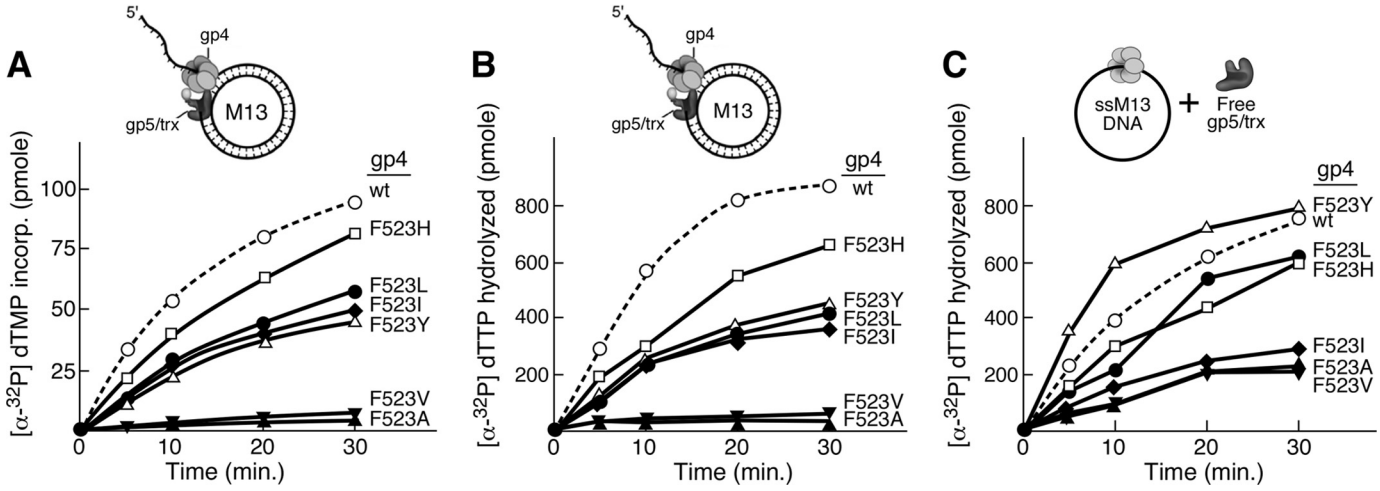

FIGURE 5. **Strand-displacement synthesis mediated by gp5/trx and gp4.** *A*, DNA synthesis mediated by gp5/trx and gp4 was measured in an assay containing 10 nM M13 dsDNA with a 5′-ssDNA tail on the interrupted strand as depicted in the *inset*, 0.5 mM dATP, dCTP, dGTP, [α-^{32}P]dTTP (1 μCi), 10 nM gp5/trx, and 20 nM hexamer of the indicated gp4. After incubation for the indicated time periods at 37 °C, DNA synthesis is expressed in terms of the quantity of [α-^{32}P]dTMP incorporated as measured by liquid scintillation counting and plotted using GraphPad Prism software. *B*, dTTP hydrolysis catalyzed by gp4 during strand-displacement DNA synthesis mediated together with gp5/trx. Reactions contained 0.5 mM dATP, dCTP, dGTP, and [α-^{32}P]dTTP (1 μCi), 5 nM M13 ssDNA, 120 nM wild-type or altered gp4 and 20 nM gp5/trx as described under "Experimental Procedures." A double-stranded M13 DNA bearing a 5′-ssDNA tail (see the *inset*) was used as a primer-template for strand-displacement synthesis as presented in *A*. The graph shows the quantity of [α-^{32}P]dTTP hydrolyzed by gp4 after the indicated time periods of incubation at 37 °C. *C*, dTTP hydrolysis catalyzed by gp4 was measured in the presence of circular M13 ssDNA. Reactions were carried out as described above.

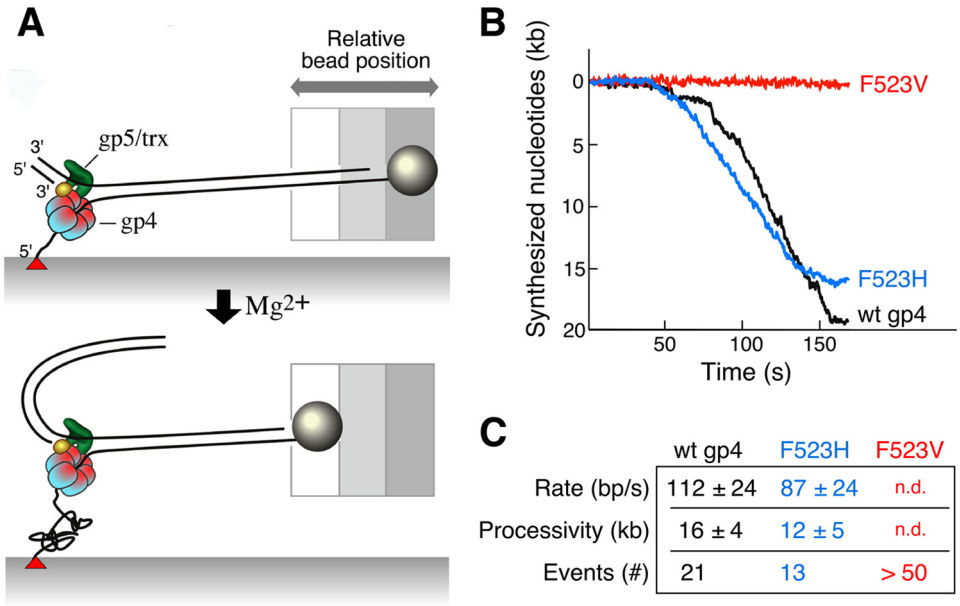

C

	wt gp4	F523H	F523V
Rate (bp/s)	112 ± 24	87 ± 24	n.d.
Processivity (kb)	16 ± 4	12 ± 5	n.d.
Events (#)	21	13	> 50

FIGURE 6. **Single-molecule analysis of strand-displacement synthesis.** *A*, λ dsDNA (48.5 kb) is attached to the surface of the flow cell via one of the 5′-ends of the fork using biotin-streptavidin interaction, the 3′-end of the same strand is attached to a paramagnetic bead using digoxigenin-antidigoxigenin interaction. T7 DNA polymerase/thioredoxin (gp5/trx) and gp4 are preassembled at the replication fork in the presence of dNTPs but in the absence of Mg^{2+}. The reaction is started by the addition of $MgCl_2$ and dNTPs. The positions of the beads are recorded and analyzed as described under "Experimental Procedures." *B*, examples of single molecule trajectories for leading strand synthesis are shown. Rate and processivity were calculated by fitting the distributions of individual single-molecule trajectories using Gaussian and exponential decay distributions, respectively. *C*, rate and processivity measurements of leading strand synthesis associated with wild-type or altered gp4. Values represent the mean ± S.E. Twenty-one events were used to calculate the rate and processivity for gp5/trx and wild-type gp4, 13 events for gp5/trx and gp4-F523H. More than 50 events were analyzed for gp5/trx and gp4-F523V mediated leading strand synthesis, but the rate and processivity could not be determined (*n.d.*).

Single-molecule analysis of strand-displacement synthesis was carried out as previously described (22, 29) and is shown schematically in Fig. 6*A*. Bacteriophage λ duplex DNA (48.5 kb) containing a replication fork is attached to a glass flow cell via the 5′-end of one strand whose 3′-end is linked to a 2.8-μm sized bead. A constant laminar flow is applied such that the resultant drag on the bead stretches the DNA molecule with a force of 3 piconewton. At this force the elasticity of the DNA is determined by entropic contributions and thus does not influence protein interactions with DNA (29). The ssDNA, due to coiling, is shorter than dsDNA at low stretching forces (<6 piconewton). Consequently, the conversion of dsDNA to ssDNA as a result of leading-strand synthesis can be monitored through a decrease in length of DNA. The change in lengths of individual DNA molecules is measured by imaging the beads and tracking their positions.

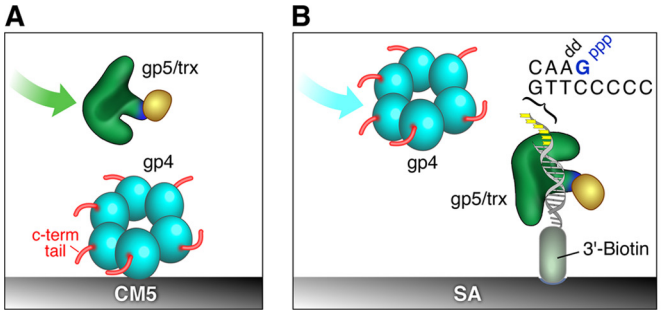

C

gp4	K_d gp5/trx (No template)	K_d gp5/trx + primer template
wt	110 ± 2	38 ± 6
F523V	150 ± 3	150 ± 6
F523H	204 ± 4	154 ± 3

FIGURE 7. **Binding of gp4 to gp5/trx.** *A*, binding of gp4 to gp5/trx in the absence of primer-template. Wild-type gp4, gp4-F523V, or gp4-F523H was immobilized in separate flow cells via their amine groups to the CM-5 sensor chip. gp5/trx was flowed over the bound gp4 as shown in the figure. Binding studies were carried out as described previously (29). Three thousand response units of gp4 are coupled to the chip, and the concentration of the gp5/trx in the flow buffer was 0.1 to 3 μM. A control flow cell lacking gp4 is used to subtract the RU resulting from nonspecific interaction. *B*, binding of gp4 to gp5/trx bound to primer-template. The primer-template DNA with biotin at the 3′ end of the template strand was immobilized on a SA-sensor chip. Binding studies were carried out as described previously (29). One hundred response units of the biotinylated primer-template were coupled to the surface. gp5/trx was injected at a concentration of 0.2 μM in a flow buffer containing 1 mM dGTP and 10 μM ddATP: a saturating 1:1 binding condition between gp5/trx and primer-template. The 100 response units resulting from the coupling of the primer-template was subtracted from the baseline. gp4 was injected at a concentration of 0.7 μM (monomer) in flow buffer containing 0.1 mM ATP and 2 mM dGTP. *C*, data shows the affinity of gp4 with gp5/trx in terms of K_d (nM) in the absence or presence of primer-template.

In the present experiment the bound DNA was preincubated with T7 DNA polymerase/thioredoxin (gp5/trx) and T7 gp4 with the four dNTPs but in the absence of Mg^{2+} for 15 min. The flow cell was then washed with 3 flow cell volumes of buffer containing the dNTPs. DNA synthesis was initiated by introducing buffer containing dNTPs and $MgCl_2$. Examples of single molecule trajectories for leading strand synthesis obtained with wild-type gp4, gp4-F523H, and gp4-F523V are shown (Fig. 6*B*). With wild-type gp4 and gp5/trx, leading strand synthesis proceeded at a rate of 112 ± 24 bp/s (n = 21) with a processivity of 16 ± 4 kbp (Fig. 6*C*), in good agreement with previous results (22, 29, 30). gp4-F523H was also able to support strand-displacement synthesis with a rate of 87 ± 24 bp/s (n = 13) and a processivity of 12 ± 5 kbp. Unlike gp4-K467A, as described above, gp4-F523V did not support strand-displacement synthesis in these experiments. We have analyzed more than 50 events for the gp4-F523V-mediated strand-displacement synthesis, however, none of them showed a considerable bead movement. In similar reaction conditions gp4-F523A also behaved like gp4-F523V (data not shown). These single molecule results support the data obtained with the ensemble experiments.

Interaction of gp4 with T7 Gp5/trx—Gene 4 protein and T7 gp5/trx have multiple modes of interaction (30). In one mode the acidic C-terminal tail of gp4 interacts with two basic loops located in the thioredoxin-binding domain of T7 DNA polymerase. This electrostatic mode captures DNA polymerase that may dissociate from the primer-template and delivers it back to the primer. When T7 gp5/trx is in a polymerizing mode, gp4 forms a complex of high affinity that does not require the electrostatic mode. To find out whether the lack of support by gp4-F523V in leading strand synthesis is not associated with its inability to interact with gp5/trx, we measured the binding of altered gp4s (gp4-F523V and gp4-F523H) to T7 gp5/trx both in the absence and presence of DNA using surface plasmon resonance.

In the absence of DNA gp4 was bound to a CM5 chip and gp5/trx flowed over the bound gp4 (Fig. 7*A*). In the presence of a primer-template, the primer-template was attached to a SA chip and gp5/trx was flowed over the bound primer-template in the presence of a dideoxynucleoside triphosphate complementary to the first nucleotide in a template position. This procedure essentially locks the polymerase into a polymerizing mode (30). Then gp4 is flowed over the polymerase, primer-template complex, and the change in surface plasmon resonance was measured (Fig. 7*B* and supplemental Fig. S6). The binding of gp4 with gp5/trx is tighter in the presence of primer-template as compared with its absence (30). As expected, in our experiments, wild-type gp4 bound to the gp5/trx with a K_D of 110 and 38 nM in the absence and presence of primer-template, respectively (Fig. 7*C*). Unlike wild-type gp4, the binding of the gp4-F523H or gp4-F523V with T7 gp5/trx did not change significantly in the absence or presence of the primer-template (Fig. 7*C*). Although there is a difference between the binding of wild-type gp4 and altered gp4 with gp5/trx in the presence of primer-template, the difference cannot be attributed to the defect of gp4-F523V for its inability to support strand-displacement synthesis because in such an experiment we did not observe any significant difference in the binding of gp4-F523H or gp4-F523V with gp5/trx.

DISCUSSION

The helicase encoded by bacteriophage T7 is a multifunctional protein that plays an essential role in unwinding dsDNA to provide a template for T7 DNA polymerase on the leading strand. Structural studies of several hexameric helicases suggest a general model by which DNA binding loops move within the central channel of the functional hexamer as a function of the NTP hydrolysis cycle (36). Despite the differences in the nucleotide-binding site architecture of hexameric helicases from SF IV (T7 gp4, *E. coli* DnaB, and T4 gp41), and AAA+ ATPases (MCM, BPV E1), these enzymes appear to translocate on ssDNA using a mechanism involving the sequential hydrolysis of NTP. It has been hypothesized that during the unwinding of duplex DNA, the translocation of these ring helicases on one strand of DNA excludes the complementary strand from its central channel (37–39). The hexameric helicases require dsDNA bearing 5′- and 3′-ssDNA tails; T7 helicase cannot ini-

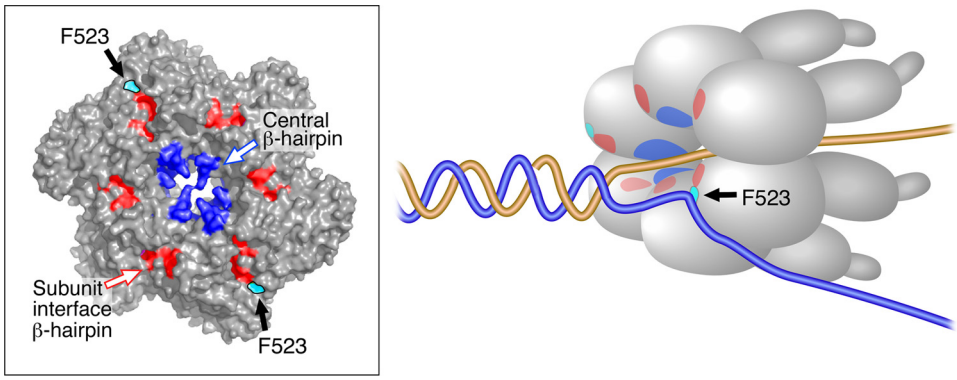

FIGURE 8. **DNA unwinding by hexameric gp4.** The schematic depicts the unwinding of a replication fork by the T7 helicase/primase. During DNA unwinding, gp4 interacts with 1 ssDNA at the center of the ring with the help of residues at central β-hairpins, whereas excluding the complementary strand by Phe^{523} from the outer surface. The *inset* shows the location of central β-hairpins (*blue*) and subunit-interface β-hairpins (*red*) in the crystal structure of the helicase domain of T7 gp4 (PDB code 1E0J) drawn on the surface view by PyMOL. The schematic also shows the location of these β-hairpins in the hexameric helicase while unwinding a replication fork. The orientation of Phe^{523} (*cyan*) toward the outer surface can be seen only from the interfaces with the empty state of NTP-binding site. Phe^{523} in other sites are buried in the structure and are not visible in the outer surface.

tiate unwinding on either a blunt end DNA or a DNA with only one ssDNA tail (16–18, 40). However, it is not known if the excluded strand interacts with the surface of the helicase. In this study, we have examined an amino acid, phenylalanine 523, on the surface of T7 DNA helicase that undergoes conformational changes upon changes in the state of hydrolysis of dTTP and that has the potential to contact the DNA.

Previous reports identified residues responsible for coupling nucleotide hydrolysis with the unwinding of DNA (20–22). These residues lie in proximity to the nucleotide-binding sites located at the interfaces of the subunits of the hexamer. From the crystal structure of T7 DNA helicase, we identified a β-hairpin structure located at the subunit interface that shows a difference in conformation based on the presence of a nucleotide in the nucleotide-binding site. The β-hairpin commences at Arg^{522} (arginine finger), which makes contact with the γ-phosphate of the bound nucleotide. Once hydrolysis takes place, Arg^{522} is displaced from the active site and probably makes contact with Glu^{348} on the adjacent subunit. In the process, the rest of the β-hairpin undergoes a conformational change, positioning itself toward the exterior surface of the protein. Phe^{523} lies at the tip of this β-hairpin and is thus in a position to interact with DNA (Fig. 1). This phenomenon is analogous to the central β-hairpin in gp4, where His^{465} acts as a phosphate sensor and plays an important role in conveying the occupancy of the nucleotide in the subunit interface to the ssDNA-binding site at the center of the ring, this communication facilitates ssDNA-dependent stimulation of dTTP hydrolysis (22).

Our results show that substituting alanine or valine for Phe^{523} results in defective coupling of dTTP hydrolysis to unwinding of dsDNA. These altered helicases retain >20% of the wild-type level of dTTP hydrolysis activity. The reduced dTTP hydrolysis activity may be due to their relatively weak ability to form hexamers and thus low affinity for ssDNA in the reactions as evidenced by the ligand-dependent oligomerization assays, and the effect of ssDNA on dTTP hydrolysis. The order of DNA unwinding activity by helicases with substitutions for Phe^{523} are gp4-F523I ≤ gp4-F523L = gp4-F523Y ≤ gp4-F523H. This order of unwinding is the exact opposite of their ability to hydrolyze dTTP in the presence of M13 ssDNA. Isoleucine can substitute for Phe^{523} in ssDNA-dependent dTTP hydrolysis activity. However, the gp4-F523I binds to dsDNA 8-fold less tightly than wild-type gp4, presumably the explanation for its low rate of unwinding activity. The rate of DNA unwinding increases with an increase in the size of the functional group from isoleucine or leucine to tyrosine and histidine. This order also correlates well with their binding affinity to dsDNA. Thus, gp4-F523H retains 70% of the wild-type level of unwinding activity despite having only 30% dTTPase activity. gp4-F523H thus efficiently couples dTTP hydrolysis to the unwinding of dsDNA. Compared with wild-type gp4, gp4-F523H exhibits a 2-fold higher efficiency in coupling dTTP hydrolysis with unwinding. However, wild-type gp4 performs an overall higher rate of unwinding. Taken together, these results suggest that Phe^{523} plays a role in coupling the energy released from the hydrolysis of dTTP to the unwinding of duplex DNA.

On the basis of our results and the crystal structure analysis, we propose that Phe^{523} interacts with the excluded strand (Fig. 8). We speculate that in the process of DNA unwinding at a replication fork one strand passes through the central channel by making interactions with the residues in the central β-hairpins, whereas the excluded strand interacts with the outer parts of the ring through Phe^{523} of the subunit-interface β-hairpins. These contacts can possibly rotate the two ssDNA strands with respect to each other and facilitate destabilizing the duplex DNA. The ssDNA, passing through the central channel, is transferred from one subunit to the adjacent one parallel with the sequential hydrolysis of NTP around the ring. However, it remains to be determined if the excluded strand is passed from one subunit to another using Phe^{523} on each of the subunits. A recent report on the mechanism of DNA unwinding by MCM helicase demonstrates that the excluded strand makes contact with the exterior surface of the ring and wraps around the outer surface to provide stability to the DNA helicase complex for an efficient unwinding (41). We also examined the ability of the altered helicases to interact with T7 gp5/trx to mediate strand-displacement DNA synthesis, the equivalent of leading strand DNA synthesis at a replication fork. gp4-F523A and gp4-F523V cannot catalyze the unwinding of duplex DNA despite having

considerable ssDNA-dependent dTTP hydrolysis. gp4-F523V and gp4-F523H bind equally well to T7 gp5/trx in the absence or presence of primer-template. Thus the defect of gp4-F523V for not supporting the strand-displacement synthesis is not due to its inability to interact with the T7 gp5/trx, rather the reason would be its own defect in coupling NTP hydrolysis with DNA unwinding. We propose that Phe^{523} is crucial for unwinding a duplex DNA junction ahead of polymerase during leading strand synthesis.

Acknowledgments—We thank Steven Moskowitz (Advanced Medical Graphics) and Joseph Lee for illustrations. We give special thanks to Dr. Jaya Singh for valuable suggestions on the manuscript. We are grateful to all the members of the Charles Richardson lab for helpful discussions and constructive comments.

REFERENCES

1. Richardson, C. C. (1983) *Cell* **33,** 315–317
2. Hamdan, S. M., and Richardson, C. C. (2009) *Annu. Rev. Biochem.* **78,** 205–243
3. Frick, D. N., and Richardson, C. C. (2001) *Annu. Rev. Biochem.* **70,** 39–80
4. Zhu, B., Lee, S. J., and Richardson, C. C. (2009) *J. Biol. Chem.* **284,** 23842–23851
5. Singleton, M. R., Dillingham, M. S., and Wigley, D. B. (2007) *Annu. Rev. Biochem.* **76,** 23–50
6. Egelman, E. H., Yu, X., Wild, R., Hingorani, M. M., and Patel, S. S. (1995) *Proc. Natl. Acad. Sci. U.S.A.* **92,** 3869–3873
7. Kim, D. E., Narayan, M., and Patel, S. S. (2002) *J. Mol. Biol.* **321,** 807–819
8. Tabor, S., and Richardson, C. C. (1981) *Proc. Natl. Acad. Sci. U.S.A.* **78,** 205–209
9. Singleton, M. R., Sawaya, M. R., Ellenberger, T., and Wigley, D. B. (2000) *Cell* **101,** 589–600
10. Crampton, D. J., Mukherjee, S., and Richardson, C. C. (2006) *Mol. Cell* **21,** 165–174
11. Liao, J. C., Jeong, Y. J., Kim, D. E., Patel, S. S., and Oster, G. (2005) *J. Mol. Biol.* **350,** 452–475
12. Johnson, D. S., Bai, L., Smith, B. Y., Patel, S. S., and Wang, M. D. (2007) *Cell* **129,** 1299–1309
13. Donmez, I., and Patel, S. S. (2006) *Nucleic Acids Res.* **34,** 4216–4224
14. Donmez, I., and Patel, S. S. (2008) *EMBO J.* **27,** 1718–1726
15. Matson, S. W., and Richardson, C. C. (1983) *J. Biol. Chem.* **258,** 14009–14016
16. Matson, S. W., Tabor, S., and Richardson, C. C. (1983) *J. Biol. Chem.* **258,** 14017–14024
17. Ahnert, P., and Patel, S. S. (1997) *J. Biol. Chem.* **272,** 32267–32273
18. Kaplan, D. L. (2000) *J. Mol. Biol.* **301,** 285–299
19. Galletto, R., Jezewska, M. J., and Bujalowski, W. (2004) *J. Mol. Biol.* **343,** 101–114
20. Washington, M. T., Rosenberg, A. H., Griffin, K., Studier, F. W., and Patel, S. S. (1996) *J. Biol. Chem.* **271,** 26825–26834
21. Crampton, D. J., Guo, S., Johnson, D. E., and Richardson, C. C. (2004) *Proc. Natl. Acad. Sci. U.S.A.* **101,** 4373–4378
22. Satapathy, A. K., Kochaniak, A. B., Mukherjee, S., Crampton, D. J., van Oijen, A., and Richardson, C. C. (2010) *Proc. Natl. Acad. Sci. U.S.A.* **107,** 6782–6787
23. Mendelman, L. V., Notarnicola, S. M., and Richardson, C. C. (1993) *J. Biol. Chem.* **268,** 27208–27213
24. Notarnicola, S. M., Park, K., Griffith, J. D., and Richardson, C. C. (1995) *J. Biol. Chem.* **270,** 20215–20224
25. Crampton, D. J., Ohi, M., Qimron, U., Walz, T., and Richardson, C. C. (2006) *J. Mol. Biol.* **360,** 667–677
26. Picha, K. M., and Patel, S. S. (1998) *J. Biol. Chem.* **273,** 27315–27319
27. Satapathy, A. K., and Richardson, C. C. (2011) *J. Biol. Chem.* **286,** 23113–23120
28. Satapathy, A. K., Crampton, D. J., Beauchamp, B. B., and Richardson, C. C. (2009) *J. Biol. Chem.* **284,** 14286–14295
29. Lee, J. B., Hite, R. K., Hamdan, S. M., Xie, X. S., Richardson, C. C., and van Oijen, A. M. (2006) *Nature* **439,** 621–624
30. Hamdan, S. M., Johnson, D. E., Tanner, N. A., Lee, J. B., Qimron, U., Tabor, S., van Oijen, A. M., and Richardson, C. C. (2007) *Mol. Cell* **27,** 539–549
31. Mendelman, L. V., Notarnicola, S. M., and Richardson, C. C. (1992) *Proc. Natl. Acad. Sci. U.S.A.* **89,** 10638–10642
32. Kolodner, R., and Richardson, C. C. (1977) *Proc. Natl. Acad. Sci. U.S.A.* **74,** 1525–1529
33. Stano, N. M., Jeong, Y. J., Donmez, I., Tummalapalli, P., Levin, M. K., and Patel, S. S. (2005) *Nature* **435,** 370–373
34. Lechner, R. L., and Richardson, C. C. (1983) *J. Biol. Chem.* **258,** 11185–11196
35. Lechner, R. L., Engler, M. J., and Richardson, C. C. (1983) *J. Biol. Chem.* **258,** 11174–11184
36. Enemark, E. J., and Joshua-Tor, L. (2008) *Curr. Opin. Struct. Biol.* **18,** 243–257
37. Jeong, Y. J., Levin, M. K., and Patel, S. S. (2004) *Proc. Natl. Acad. Sci. U.S.A.* **101,** 7264–7269
38. Kaplan, D. L., Davey, M. J., and O'Donnell, M. (2003) *J. Biol. Chem.* **278,** 49171–49182
39. Patel, S. S., and Picha, K. M. (2000) *Annu. Rev. Biochem.* **69,** 651–697
40. Rothenberg, E., Trakselis, M. A., Bell, S. D., and Ha, T. (2007) *J. Biol. Chem.* **282,** 34229–34234
41. Graham, B. W., Schauer, G. D., Leuba, S. H., and Trakselis, M. A. (2011) *Nucleic Acids Res.* **39,** 6585–6595